RELATIVE NAVIGATION OF FORMATION-FLYING SATELLITES

Anne LONG, David KELBEL, Taesul LEE, and Dominic LEUNG

Computer Sciences Corporation
Lanham-Seabrook, Maryland USA 20706

J. Russell CARPENTER and Cheryl GRAMLING

NASA Goddard Space Flight Center
Greenbelt, Maryland USA 20771

ABSTRACT –*This paper compares autonomous relative navigation performance for formations in eccentric, medium and high-altitude Earth orbits using Global Positioning System (GPS) Standard Positioning Service (SPS), crosslink, and celestial object measurements. For close formations, the relative navigation accuracy is highly dependent on the magnitude of the uncorrelated measurement errors. A relative navigation position accuracy of better than 10 centimeters root-mean-square (RMS) can be achieved for medium-attitude formations that can continuously track at least one GPS signal. A relative navigation position accuracy of better than 15 meters RMS can be achieved for high-altitude formations that have sparse tracking of the GPS signals. The addition of crosslink measurements can significantly improve relative navigation accuracy for formations that use sparse GPS tracking or celestial object measurements for absolute navigation.*

1 – INTRODUCTION

The Guidance, Navigation, and Control Center (GNCC) at Goddard Space Flight Center (GSFC) has successfully developed high-accuracy autonomous satellite navigation systems using the National Aeronautics and Space Administration's space and ground communications systems and the Global Positioning System (GPS). In addition, they have demonstrated an autonomous navigation capability using real Sun and Earth horizon measurements [Long 00]. The GNCC has leveraged this experience to develop advanced spacecraft systems that provide autonomous navigation and control of formation flyers in a wide range of orbits.

To support this effort, the GNCC is assessing the absolute and relative navigation accuracy achievable for proposed formations using GPS, crosslink, ground-to-satellite Doppler, and celestial object sensor measurements. This paper summarizes the results from high-fidelity simulations that were performed to study two proposed formation-flying missions. One formation consists of four satellites maintained in medium-altitude Earth orbits (MEOs) of approximately 500 by 7000 kilometer altitudes. The other formation is based on the initial phase of the Magnetospheric Multiscale (MMS) mission, which consists of four satellites in high-altitude Earth orbits (HEOs) of approximately 1.2 by 12 Earth radii. This paper quantifies the relative navigation accuracy achievable for each of these formations as a function of the tracking measurement types and their quality. This research was supported by the NASA Space Operations and Management Office.

2 – RELATIVE NAVIGATION CONCEPTS

Relative navigation accuracy is a function of the navigation algorithm and the tracking measurement type, quality, and frequency. The "best" choice for a specific mission depends on the orbital type and the relative accuracy requirements. GPS tracking is an attractive choice for Earth orbiters that are within range of the GPS signal. Crosslink (i.e., between satellites in the formation),

ground-station-to-satellite Doppler, and celestial object (e.g. line-of-sight (LOS) to a planet or angle between a star and a planet) measurements can be used regardless of the satellite altitude.

The absolute state covariance for satellite i is approximately

$$E\left[\Delta \overline{X}_i (\Delta \overline{X}_i)^T\right] = P_i = P_i^{dynamic} + P_i^{measurement} \tag{1}$$

where $P_i^{dynamic}$ is the absolute state covariance due to dynamic errors, which arise primarily from the mismodeling of the satellite perturbations; and $P_i^{measurement}$ is the absolute state covariance due to measurement-related error sources, which can include receiver/sensor noise and biases, signal propagation delays, and errors in the transmitter's location and the signal transmission time. The relative state covariance for satellites i and j is approximately

$$E\left[\left(\Delta \overline{X}_i - \Delta \overline{X}_j\right)\left(\Delta \overline{X}_i - \Delta \overline{X}_j\right)^T\right] = P_i^{relative} = P_i + P_j - P_{ij} - \left(P_{ij}\right)^T \tag{2}$$

where P_i and P_j represent the absolute state covariance of satellites i and j and P_{ij} represents the cross-correlation-covariance that develops due to common measurement biases, common model errors, or common process noise. [Carp 02] discusses the impact of correlated errors on the relative state errors in more detail.

For satellites using GPS for navigation, the absolute state vector computation can be performed using either an instantaneous point solution method or a real-time filtered algorithm. The analysis presented in [Lon2 00] indicates that relative navigation by differencing absolute state vectors obtained using the point solution method is not suitable for continuous real-time navigation of formations of satellites in orbits for which fewer than six GPS Space Vehicles (SVs) are visible during significant portions of the orbit. In addition, because point solutions do not provide accurate velocity estimates, they are not suitable for applications in which state vector information must be predicted ahead in time, e.g., to support autonomous maneuver planning.

A high-fidelity real-time filtered algorithm, such as that implemented in the GPS Enhanced Onboard Navigation System (GEONS) [Godd 00], reduces the impact of the measurement errors by using an extended Kalman filter in conjunction with an accurate orbital dynamics model. In addition to the differencing of independently-estimated state vectors, the real-time filtered approach can support simultaneous estimation of the state vectors of all satellites in the formation.

Table 1 lists the major absolute and relative error sources for the measurement types considered in this study. The strategy for improving the absolute navigation accuracy is to reduce the impact of the major dynamic and measurement errors. Although dynamic mismodeling can be the dominant absolute error source, similar satellites flying in close formations have common dynamic model errors that do not contribute significantly to relative errors. Therefore, to improve relative navigation accuracy, the effect of uncorrelated (i.e. not common) measurement errors must be minimized by reducing the error contribution from receiver/sensor noise and biases and by limiting GPS measurements to only GPS SVs common to all satellites in the formation.

Table. 1. Major Absolute and Relative Error Sources

Error Source	Absolute Error Contribution	Relative Error Contribution
Spacecraft Dynamic Perturbation Models	Yes	No, for similar satellites in close formations
Transmitter Ephemeris and Clock (e.g. GPS SV)	Yes	No, for simultaneous measurements from common transmitters
		Yes, for measurements from noncommon transmitters
Signal Propagation Delays (e.g. ionospheric delays)	Yes	No, for simultaneous measurements from common transmitters to spacecraft in close formations
		Yes, for measurements from noncommon transmitters
Receiver/sensor Measurement Noise	Yes	Yes
Receiver/sensor Measurement Bias (e.g. receiver clock bias, sensor misalignment)	Yes	Yes

Approaches for reducing the impact of uncorrelated errors include (1) estimation of the relative state using differenced GPS pseudorange measurements and/or crosslink measurements between spacecraft in the formation, (2) receiver/sensor improvements to reduce measurement noise (e.g., use of carrier-smoothed pseudorange and/or carrier phase measurements) and to reduce biases (e.g., more accurate clocks), and (3) adjustment of the estimation parameters (e.g., measurement standard deviation versus filter state process noise magnitudes).

Previously, the authors investigated relative navigation performance using standard GPS pseudorange, singly-differenced GPS pseudorange, and crosslink measurements [Kelb 01]. Using GPS pseudorange from a typical space receiver with an ultra-stable frequency reference without selective availability enabled, the more complex algorithms using singly-differenced and one-way crosslink pseudorange provided relative navigation performance comparable to that achieved by differencing independently-estimated absolute solutions using signals from only common GPS SVs. Only the addition of crosslink round-trip range measurements was found to significantly improve relative navigation accuracy for formations with sparse tracking of the GPS signals. This paper evaluates the impact of receiver/sensor improvements and adjustment of the estimation parameters on the relative navigation accuracy for the same MEO and HEO formations using GPS pseudorange, crosslink, and/or celestial object measurements.

3 – PERFORMANCE SIMULATION PROCEDURE

Realistic simulations were performed for two representative formations. The MEO formation consists of four satellites maintained in Earth orbits at an inclination of 80 degrees with altitudes of approximately 500 kilometers by 7000 kilometers. The orbital period is approximately 3 hours. All satellites have nearly identical surface areas of 0.6613 meters^2 and masses of 200 kilograms. The intersatellite separations in this tetrahedral formation range from 10 kilometers at apogee to 30 kilometers at perigee, with three satellites in the same orbit plane and one out of plane. The HEO formation consists of four satellites maintained in 1.2-Earth-radii by 12-Earth-radii orbits at an inclination of 10 degrees, with an orbital period of 1 day. All satellites have nearly identical surface areas of 1.12 meters^2 and masses of 220 kilograms. The intersatellite separations in this tetrahedral formation range from 10 kilometers at apogee to 150 kilometers at perigee, with planar separations of less than 0.1 degree.

Realistic GPS pseudorange, crosslink range and LOS, and celestial object measurements were simulated using high-fidelity truth ephemerides generated using the Goddard Trajectory Determination System (GTDS) with a high-accuracy force model, which included a Joint Gravity Model (JGM) for nonspherical gravitational forces, Jet Propulsion Laboratory Definitive Ephemeris 200 for solar and lunar gravitational forces, atmospheric drag, and solar radiation pressure forces. GTDS is the primary orbit determination program used for operational satellite support at GSFC.

The GPS signal strength at the GPS receiver's location was modeled assuming the nominal GPS Block II signal antenna pattern (including both the main and side lobes). Each MEO satellite had one hemispherical GPS antenna, with a zenith-pointing boresight. Each HEO satellite had identical hemispherical antennas, pointing in the zenith and nadir directions. The GPS SV signal attenuation model that was used provides realistic signal acquisition predictions [More 00]. The number of simultaneous measurements was not restricted. Fig. 2 illustrates the geometry of the MEO and HEO satellites with respect to the primary and first side lobe of the signal of a single GPS SV.

Fig. 3 shows the number of GPS SVs as a function of time that can be acquired and tracked by a standard GPS receiver (i.e. 35-dB-Hertz threshold) on the MEO and a reduced threshold (i.e. 30 dB-Hertz) receiver on the HEO. The 30-dB-Hertz tracking threshold can be achieved if the receiver employs weak signal tracking strategies to track the weaker signals in the side lobes of the GPS antenna pattern [More 00]. In both cases, the largest number of GPS SVs is visible at perigee. The MEO satellite's single zenith-pointing hemispherical antenna considerably limits GPS visibility at high altitudes. For the HEO formation, a nadir-pointing high gain GPS antenna would further improve GPS signal acquisition and tracking at high altitudes.
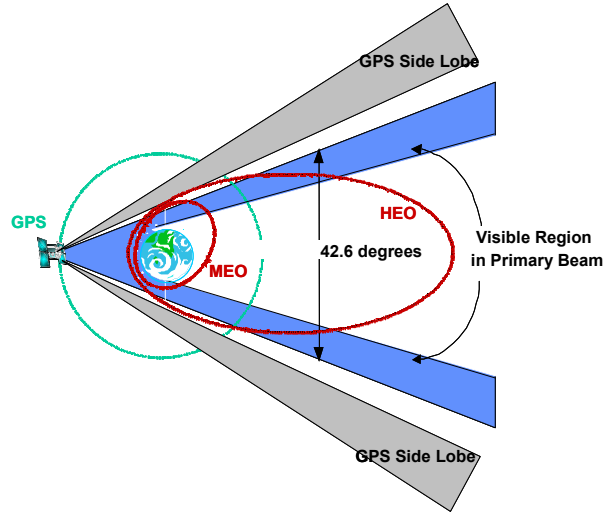
Fig. 2 GPS Tracking Geometry
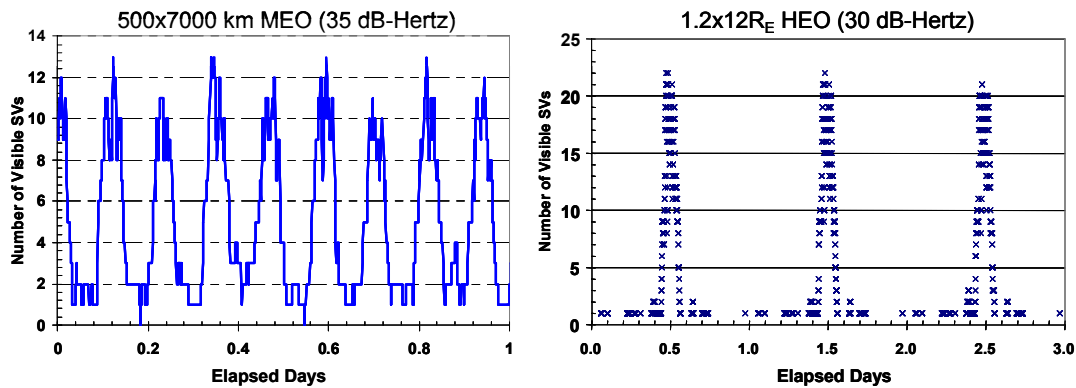
Fig. 3 GPS SV Visibility as a Function of Time

GPS SV ephemeris and clock errors were applied at a 2-meter (1-sigma) level, using the Lear4 autoregressive integrated moving average time series model (JSC 93). Ionospheric delays were included. A twice-integrated random walk model, based on [Brow 97], was used to simulate the receiver clock bias and clock drift noise contributions to the GPS measurement errors, consistent with the characteristics of either a rubidium-quality ultra-stable oscillator (USO) or temperature-compensated crystal oscillator (TCXO). The crosslink remote-to-local (1-way) range measurements were biased by the difference between the simulated transmitter and receiver clock biases. The simulated crosslink round-trip range measurements were not biased.

Satellite-to-Sun and satellite-to-Earth LOS measurements were simulated for the MEO formation assuming a sensor performance consistent with a state-of-the-art fine pointing sun sensor and an attitude accuracy of 1 arc minute. Crosslink LOS measurements, based on the vision-based system discussed in [Alon 01], were simulated assuming an optical sensor and an attitude accuracy of 1 arc minute. Measurements of the angle between a Northern star and the Sun or the Earth were simulated consistent with the characteristics of an optical sensor.

The extended Kalman filter algorithm available in GEONS was used to process these measurement sets. Atmospheric drag and solar radiation pressure forces were included in the state propagation using atmospheric drag and solar radiation pressure coefficients that were offset by 10 percent and 5 percent respectively from the values used in the truth ephemeris generation. Monte Carlo simulations were performed for each formation to quantify the expected distribution in the absolute and relative solution errors as a function of variations in the random GPS measurement errors. The following error statistics were accumulated for the ensemble of solutions obtained by processing 25 sets of simulated GPS pseudorange measurements that were created by varying the random number seeds used for the GPS ephemeris and clock, receiver clock, and random measurement errors:

- Ensemble RMS/maximum error, which is the RMS/maximum of the true error (difference between the estimated and true states) at each time computed across all Monte Carlo solutions.
- Steady-state time-wise ensemble RMS/maximum error, which is the RMS/maximum of the ensemble true errors computed along the time axis, omitting the initial convergence period.

4 – RELATIVE NAVIGATION PERFORMANCE FOR ECCENTRIC MEO FORMATION

The MEO formation lies well below the GPS constellation altitude, with continuous visibility of at least one GPS SV. Fig. 4 compares the absolute and relative position accuracy (in terms of the steady-state time-wise ensemble RMS) as a function of the GPS pseudorange noise and the receiver clock quality for solutions obtained by independently estimating the absolute satellite states. The random noise levels of 2, 0.25, and 0.02 meters correspond to standard pseudorange, carrier-smoothed pseudorange, and carrier phase measurements, respectively. Fig. 5 shows the ensemble RMS and maximum absolute and relative position errors over the 2-day estimation time span followed by a 1-day prediction time span, from the Monte Carlo simulation using GPS pseudorange measurements with 0.02 meter noise and an USO.
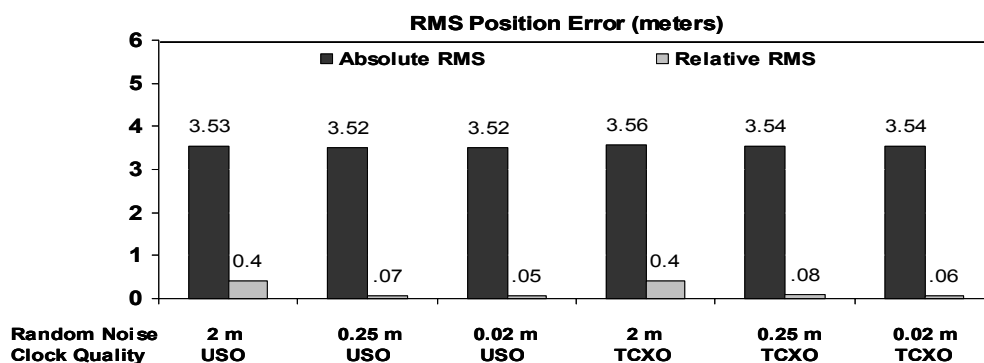

Fig. 4. Ensemble Absolute and Relative Position RMS Errors for MEO Formation
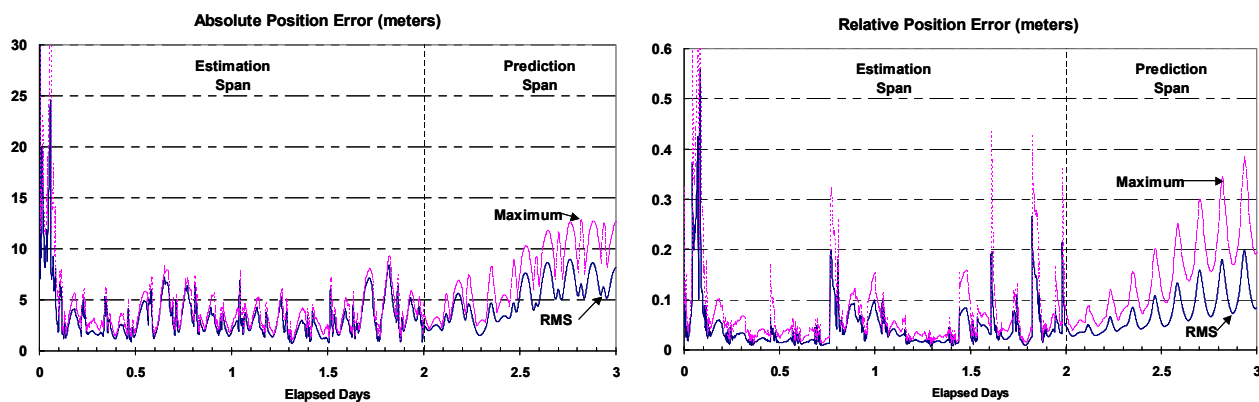Using GPS Pseudorange Measurements

Fig. 5. Ensemble Absolute and Relative Position Errors for MEO Formation
Using Carrier-Phase-Quality GPS Measurements

The estimation process reached steady state immediately following the second perigee passage. The variation in the absolute and relative error statistics for all satellites in the formation was small. The steady-state time-wise ensemble RMS of the absolute errors were approximately 3.5 meters position, 1.75 millimeters per second velocity, and 8 meters (0.03 microseconds) clock bias, nearly independent of the receiver noise, clock quality, and adjustment of the filter state process noise parameters. The maximum errors occur following apogee. For the Monte Carlo simulation, the maximum absolute errors encountered were approximately 9.5 meters, 7.0 millimeters per second velocity, and 28 meters (0.1 microsecond) for an USO and 110 meters (0.4 microseconds) for a

TCXO. The primary sources of the absolute navigation error are dynamic modeling errors, unmodeled ionospheric delay, GPS SV ephemeris and clock errors, and receiver clock errors.

When the absolute solutions are differenced, the error contributions from correlated errors cancel and the relative navigation accuracy is significantly better than the absolute errors. Since the satellites are in tight formation in nearly the same orbits and track common GPS SVs 99.8 percent of the time, the absolute error contributions from dynamic errors, ionospheric delay, and GPS SV ephemeris and clock errors are highly correlated and nearly cancel in all of these cases. The primary contributors to the relative navigation error are the uncorrelated measurement noise and receiver clock errors. The reduction in the relative errors achieved by reducing the random noise levels was found to be very sensitive to the magnitude of the clock state process noise. With carrier-phase-quality pseudoranges (0.02 m noise with an USO), the Monte-Carlo simulations yielded a steady-state time-wise ensemble RMS relative accuracy of approximately 0.05 meters in position and 0.03 millimeters per second in velocity, with maximums below 0.45 meters in position and 0.27 millimeters per second in velocity.

A previous study by the authors [Kelb 01] indicated that the processing of one-way crosslink range in addition to standard GPS pseudorange (of comparable accuracy) does not improve the absolute or relative accuracy. However, the addition of round-trip crosslink range yielded a reduction of about 25 percent in the relative navigation error. Recent simulations evaluated improvement in relative performance when crosslink range and crosslink LOS measurements are processed in addition to celestial object measurements, which have significantly larger noise and uncorrelated biases than the GPS measurements. Fig. 6 summarizes the resulting steady-state absolute and relative error statistics. In these simulations, both the absolute and relative errors are dominated by the uncorrelated measurement errors (1 arc minute noise and 0.2 arc minute bias for LOS measurements to the Sun or Earth and 0.1 arc minute noise and 0.01 arc minute bias for measurements of the angle between a Northern star and the Sun or the Earth). The addition of only crosslink range (2 meter noise) or crosslink LOS (1 arc minute noise and 0.2 arc minute bias) significantly reduced the relative navigation errors. However, the addition of both crosslink measurement types reduced the relative errors to below 1 meter RMS.
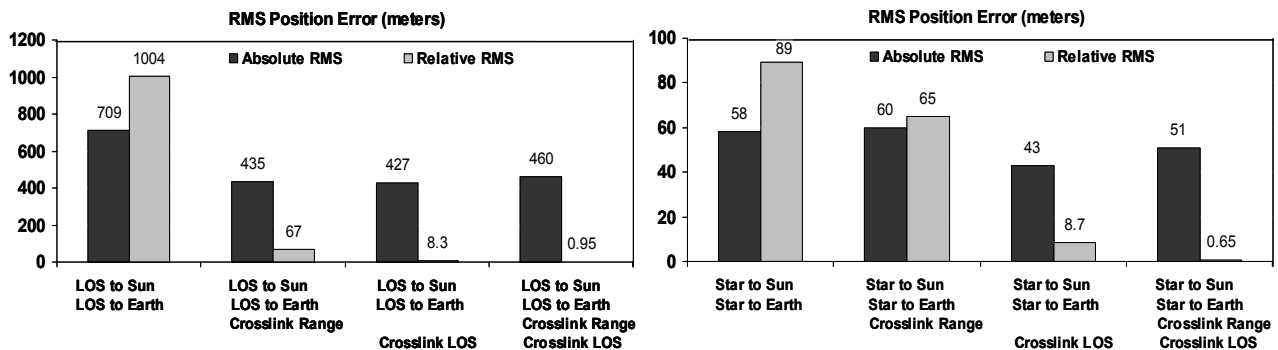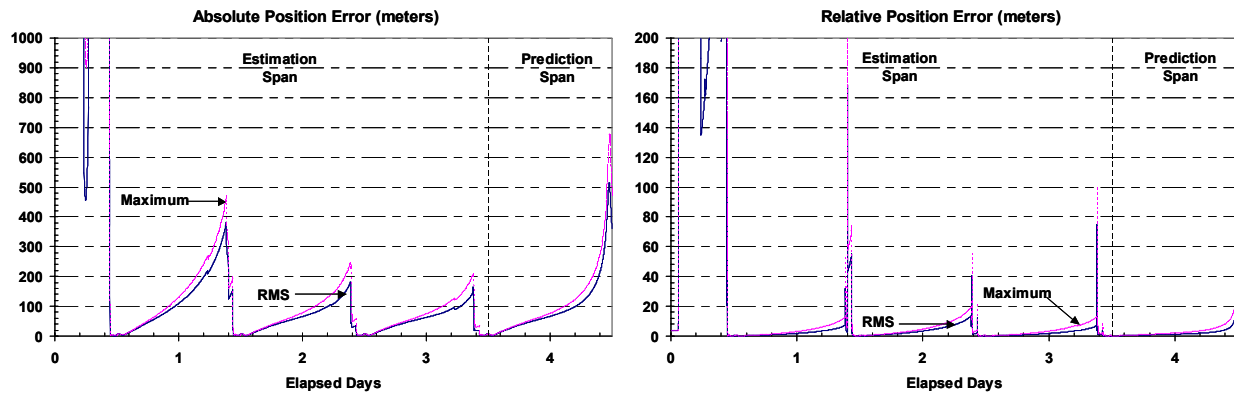

Fig. 6. Absolute and Relative Position RMS Errors for MEO Formation
Using Celestial Object and Crosslink Measurements

5 – RELATIVE NAVIGATION PERFORMANCE FOR ECCENTRIC HEO FORMATION

The HEO formation is above the GPS constellation and outside the primary beam for a large portion of its orbit. Fig. 7 compares the absolute and relative position accuracy (in terms of the steady-state time-wise ensemble RMS) as a function of the GPS measurement noise and the receiver clock quality for solutions obtained by independently estimating the absolute satellite states. Fig. 8 shows the ensemble RMS and maximum absolute and relative position errors over the 3.5-day estimation time span followed by a 1-day prediction time span, from the Monte Carlo simulation using GPS pseudorange measurements with 0.02 meter noise and an USO.
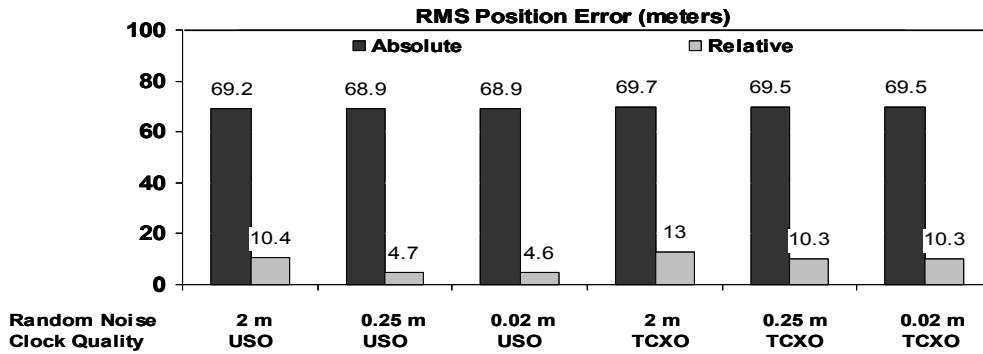
Fig. 7. Ensemble RMS Absolute and Relative Position Errors for HEO Formation Using GPS Pseudorange Measurements

Fig. 8. Ensemble Absolute and Relative Position Errors for HEO Formation Using Carrier-Phase-Quality GPS Pseudorange Measurements

The estimation process reached steady state immediately following the first perigee passage. The steady-state time-wise ensemble RMS of the absolute errors were approximately 70 meters in position and 3.8 millimeters per second in velocity, nearly independent of the receiver noise, clock quality, and adjustment of the filter state process noise parameters. The absolute RMS clock errors were 600 meters (2 microseconds) and 8 kilometers (27 microseconds) for USO and TCXO clocks, respectively, which was sensitive to the magnitude of the clock state process noise. The maximum errors occur following apogee. The maximum absolute errors encountered were approximately 280 meters in position, 21 millimeters per second in velocity, and 2.5 kilometers in clock bias for the USO and 100 kilometers in clock bias for the TCXO clocks, respectively. The primary sources of the absolute navigation error are dynamic modeling errors, unmodeled ionospheric delay, and receiver clock errors.

Since the satellites are in close formation and track common GPS SVs 98.7 percent of the time, the dynamic modeling, ionospheric delay, and GPS SV ephemeris and clock error contributions nearly cancel when the absolute state vectors are differenced. The primary contributors to the relative navigation error are the uncorrelated measurement noise and receiver clock errors. The reduction in the relative errors achieved by reducing the random noise levels was found to be very sensitive to the magnitude of the clock state process noise. With carrier-phase-quality pseudoranges (0.02 m noise with an USO), the Monte-Carlo simulations yielded a steady-state time-wise ensemble RMS relative accuracy of approximately 4.6 meters in position and 0.30 millimeters per second in velocity, with maximums below 160 meters in position and 13 millimeters per second in velocity.

Additional Monte-Carlo simulations were performed to evaluate the impact of adding crosslink measurements between the local and remote satellites. In these simulations, the processing of crosslink round-trip range (with 2 meter noise), in addition to standard GPS pseudorange measurements (2 meter noise with an USO) for both the remote and local satellites, reduced the relative position error to 3 meters RMS and 38 meters maximum. This improvement is probably

due to a reduction in the impact of the uncorrelated receiver clock biases associated with the standard GPS measurements.

6 – CONCLUSIONS AND FUTURE DIRECTIONS

This study assesses the sensitivity of the relative navigation accuracy to receiver/sensor improvements and adjustment of the estimation parameters for a 500x7000 kilometer altitude MEO and a 1.2x12 Earth radii HEO formation. For both formations using only GPS measurements, the primary factors driving the relative navigation accuracy are the frequency of acquisition and tracking of signals from common GPS SVs and the uncorrelated measurement noise and receiver clock errors.

For the MEO formation, with nearly continuous tracking of the GPS signals, the differencing of absolute state vectors can provide a RMS relative navigation accuracy of better than 0.08 meters in position and 0.05 millimeters per second in velocity using carrier-smoothed pseudorange. For the HEO formation, with continuous tracking of the GPS signals only near perigee, the differencing of absolute state vectors can provide a RMS relative navigation accuracy of better than 6 meters in position and 0.4 millimeters per second in velocity, using a GPS receiver with weak signal tracking improvements, a highly stable clock, and carrier-smoothed pseudorange. The inclusion of accurate crosslink round-trip range and/or crosslink LOS measurements was found to improve relative navigation accuracy by reducing the impact of the uncorrelated measurement errors.

The relative navigation version of GEONS has been integrated into a low cost GPS satellite receiver being developed by the GSFC GNCC. This formation-flying receiver is being used to demonstrate end-to-end performance in GNCC's formation-flying test bed.

REFERENCES

[Alon 01]   R. Alonso et al, "Relative Navigation for Formation-Flying Satellites," *Proceedings of the 2001 Flight Mechanics Symposium*, NASA Goddard Space Flight Center, Greenbelt, Maryland, June 19-21, 2001, pp. 115-129

[Brow 97]   R. G. Brown and P. Y. C. Hwang, *Introduction to Random Signals and Applied Kalman Filtering*, Third Edition, John Wiley and Sons, 1997

[Carp 02]   J. R. Carpenter, "Partially Decentralized Control Architectures for Satellite Formations," Proceedings of the 2002 AIAA Guidance, Navigation, and Control Conference, Monterey, California, August 5-8, 2002

[Godd 00]   Goddard Space Flight Center, CSC-5547-02R0UD0, Global Positioning System (GPS) Enhanced Onboard Navigation System (GEONS) Mathematical Specifications, Release 1.2, A. Long et al, prepared by Computer Sciences Corporation, July 2002

[JSC 93]   Johnson Space Flight Center, Range Bias Models for GPS Navigation Filters, William M. Lear, Charles Stark Draper Laboratory, June 1993

[Kelb 01]   D. Kelbel et al., "Evaluation of Relative Navigation Algorithms for Formation-Flying Satellites Using GPS," Proceedings of the 2001 Flight Mechanics Symposium, NASA Goddard Space Flight Center, Greenbelt, Maryland, June 19-21, 2001.

[Long 00]   A. Long et al., "Autonomous Navigation of High-Earth and Libration Point Orbiting Satellites using Celestial Objects," Paper AIAA-2000-3937, Presented at the AIAA/AAS Astrodynamics Specialist Conference, Denver , Colorado, August 14-17, 2000.

[Lon2 00]   A. Long et al., "Autonomous Relative Navigation for Formation-Flying Satellites Using GPS," Paper MS00/18, Proceedings of the International Symposium on Space Dynamics, CNES, Biarritz , France, June 26-30, 2000.

[More 00]   M. Moreau et al., "GPS Receiver Architecture and Expected Performance for Autonomous GPS Navigation in Highly Eccentric Orbits," Navigation: Journal of the Institute of Navigation, Vol.47, No. 3, Fall 2000, pp. 191-204.